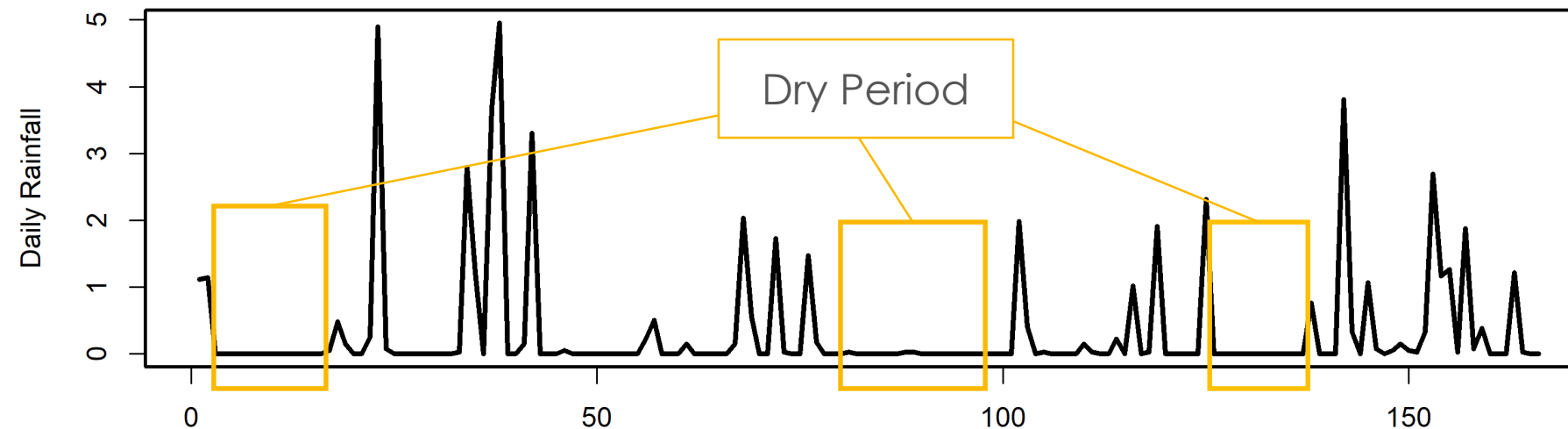




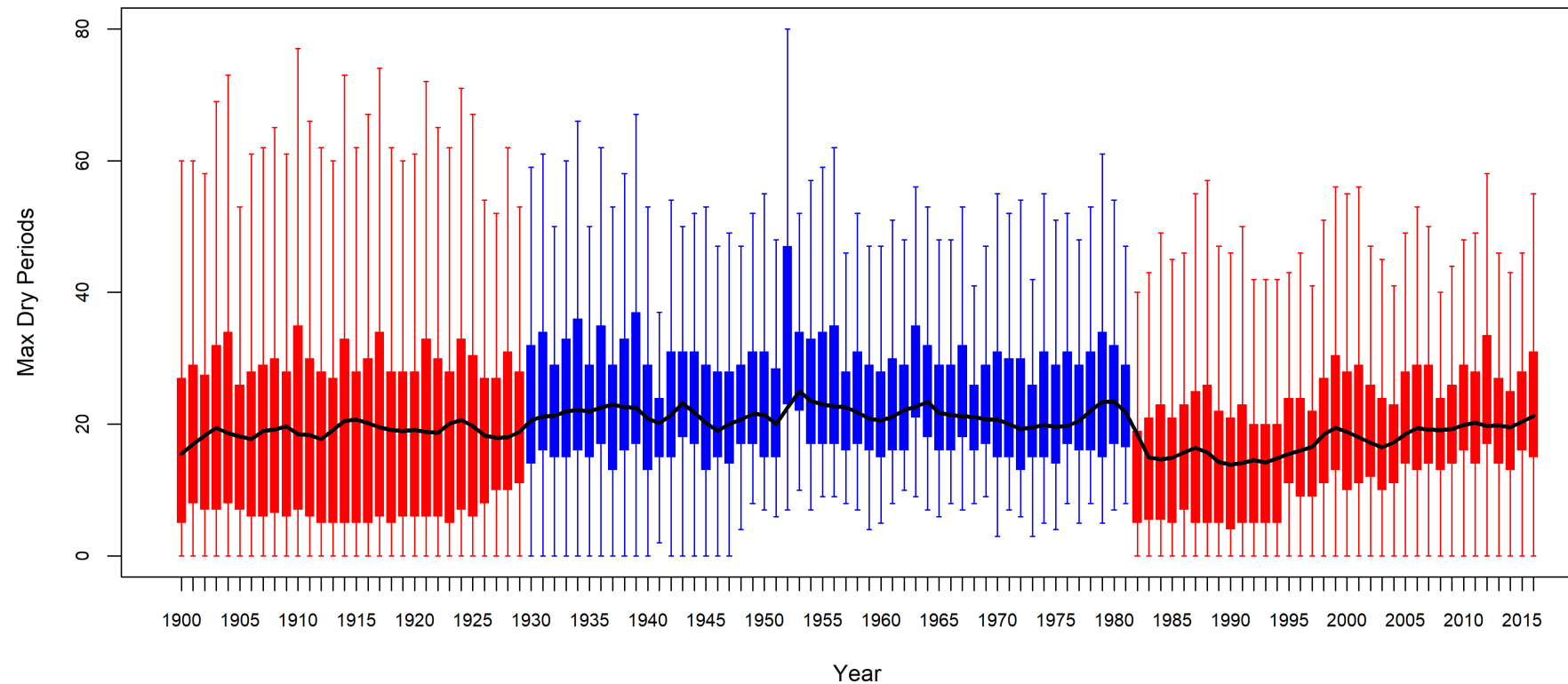
U.S. MULTI-DECADAL DRY PERIODS AND CLIMATE CONNECTION

Saman Armal, Naresh Devineni, Nir Krakauer, Reza Khanbilvardi

Department of Civil Engineering – CCNY



Precipitation
Dry Periods



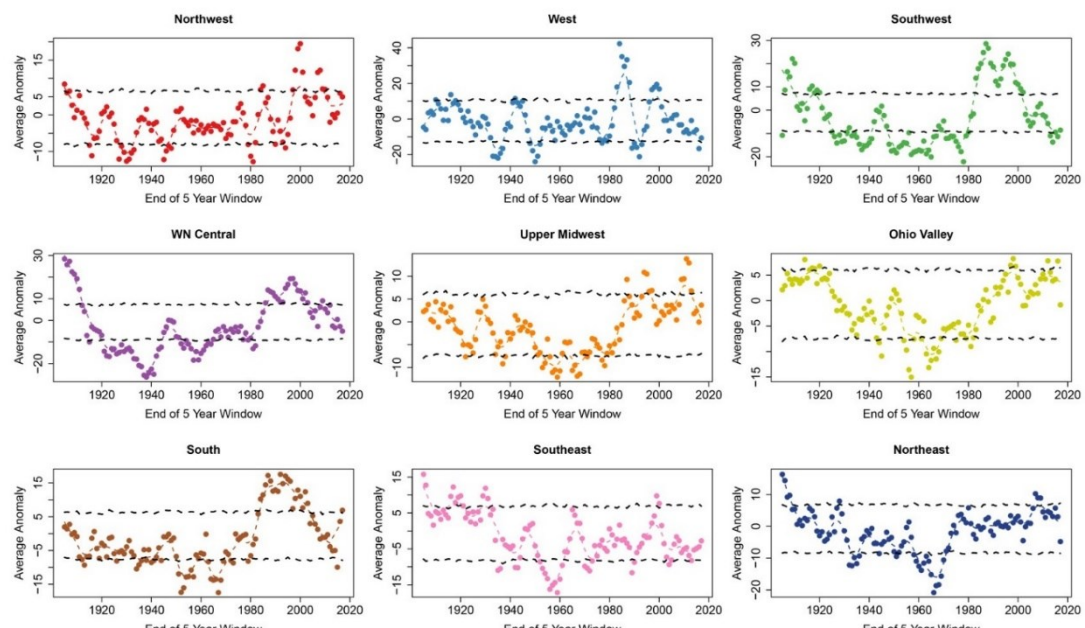
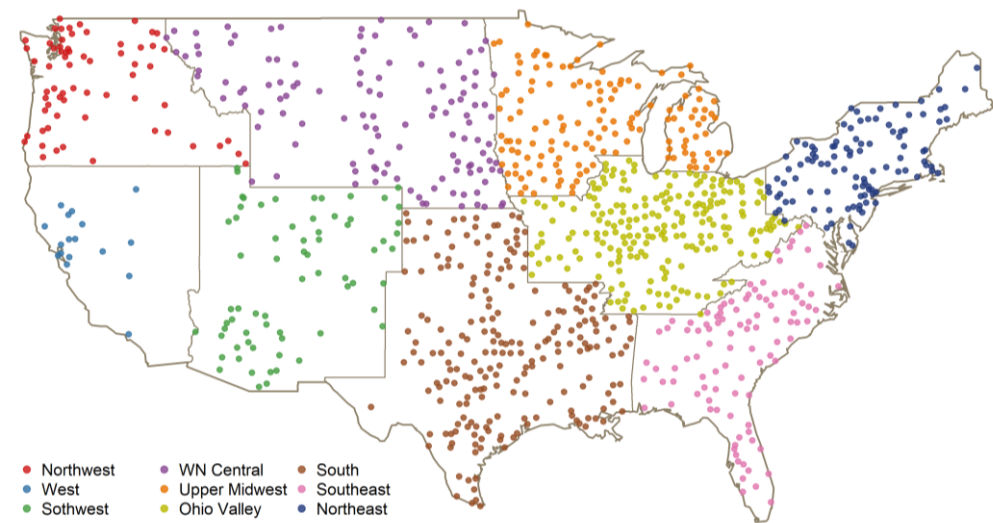
Time Variability of
United States
Maximum Dry Periods
(1900 - 2016)

Precipitation Anomalies to Confirm the Outcome of Maximum Dry Spell

Climate Region	1900	1910	1920	1930	1940	1950	1960	1970	1980	1990	2000	2010
Northwest	15	6-	18-	24-	24-	0	0	6-	15	23	38	8
West	0	15	0	29-	12-	18-	0	6-	46	24-	8	6-
Southwest	13	17	10-	16-	8-	20-	16-	18-	23	33	10	8-
WN Central	19	8	21-	24-	12-	19-	12-	5-	15	38	19	0
Upper Midwest	0	0	6-	12-	0	35-	29-	18-	10	40	10	40
Ohio Valley	0	40	10	0	12-	25-	44-	6-	12-	30	0	20
South	0	4-	0	15-	12-	27-	27-	12-	29	48	19	5
Southeast	17	33	17	17	10-	38-	10-	14-	5-	8	8	5-
Northeast	50	0	12	24-	5-	14-	48-	10-	0	0	38	0

Anomaly of Precipitation in Different Climate Regions of United States

Quantile Perturbation Method
to identify the anomalies



Wet gets Wetter, Dry Gets Drier

Robust Responses of the Hydrological Cycle to Global Warming

ISAAC M. HELD

National Oceanic and Atmospheric Administration/Geophysical Fluid Dynamics Laboratory, Princeton, New Jersey

BRIAN J. SODEN

Rosenstiel School for Marine and Atmospheric Science, University of Miami, Miami, Florida

(Manuscript received 13 September 2005, in final form 17 March 2006)

ABSTRACT

Using the climate change experiments generated for the Fourth Assessment of the Intergovernmental Panel on Climate Change, this study examines some aspects of the changes in the hydrological cycle that are robust across the models. These responses include the decrease in convective mass fluxes, the increase in horizontal moisture transport, the associated enhancement of the pattern of evaporation minus precipitation and its temporal variance, and the decrease in the horizontal sensible heat transport in the extratropics. A surprising finding is that a robust decrease in extratropical sensible heat transport is found only in the equilibrium climate response, as estimated in slab ocean responses to the doubling of CO_2 , and not in transient climate change scenarios. All of these robust responses are consequences of the increase in lower-tropospheric water vapor.

1. Introduction

There remains considerable uncertainty concerning the magnitude of the temperature response to a given increase in greenhouse gases. But there are a number of climatic responses that are tightly coupled to the temperature response. Most of these are related, directly or indirectly, to lower-tropospheric water vapor. We are confident that lower-tropospheric water vapor will increase as the climate warms. We can predict, with nearly as much confidence, that certain other changes will occur that are coupled to this increase in water vapor. In this article we describe some of these robust hydrological responses to warming.

We use the archive of coupled climate models results organized by the Program for Climate Model Diagnosis and Intercomparison (PCMDI) for the Fourth Assessment Report (AR4) of the Intergovernmental Panel on Climate Change as our primary tool in assessing robustness. Some aspects of the hydrological responses to warming are consistent among these models and some

are not. To study the latter requires one to understand the consequences of different model formulations, often at a detailed level. When studying a consistent part of the response, in contrast, one is not concerned with the specifics of individual models, but with providing simple physical arguments that add additional support for the plausibility of the response. Some of these robust responses to warming are already well appreciated, but we gather several together here, partly for pedagogical reasons, and partly with the hope of motivating new observational studies to determine whether these responses, which the models predict are already occurring, are detectable.

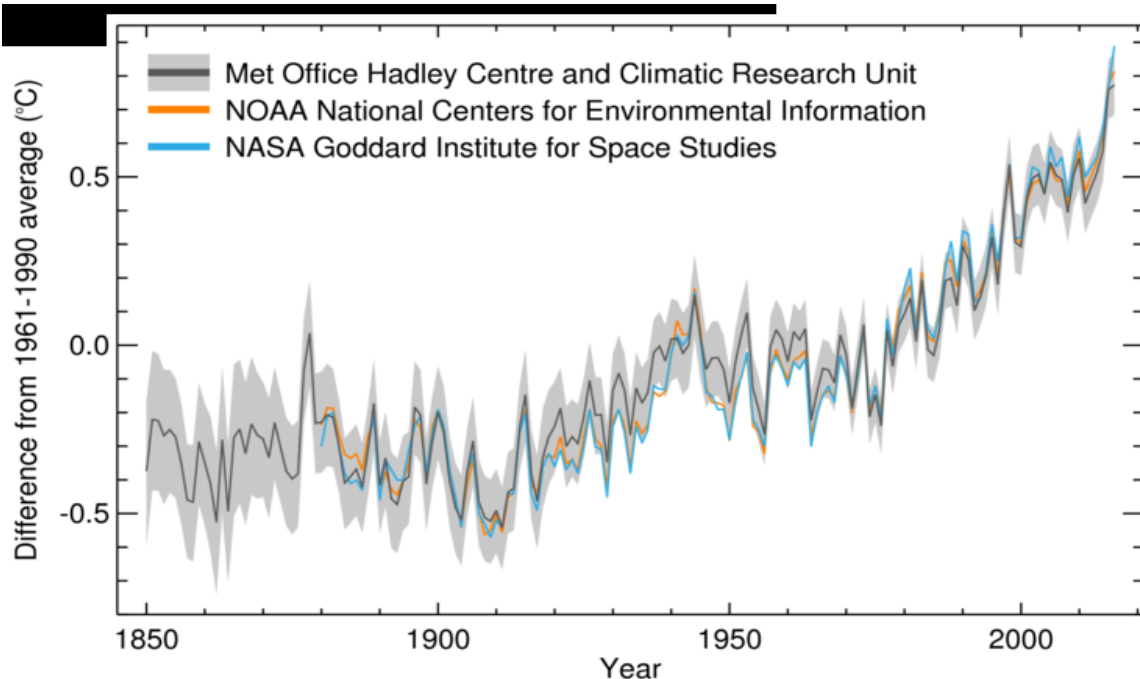
As in many discussions of water vapor and global warming, our starting point is the Clausius–Clapeyron (CC) expression for the saturation vapor pressure:

$$\frac{d \ln e_s}{dT} = \frac{L}{RT^2} \equiv \alpha(T), \quad (1)$$

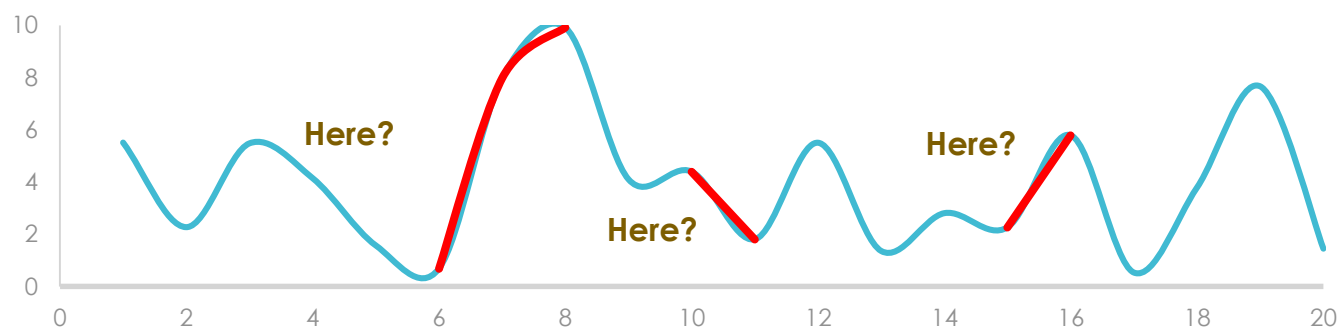
where L is the latent heat of vaporization and R is the gas constant. At temperatures typical of the lower troposphere, $\alpha \approx 0.07 \text{ K}^{-1}$; the saturation vapor pressure increases by about 7% for each 1-K increase in temperature. If the equilibrium response of lower-tropospheric temperatures to a doubling of CO_2 is close to the canonical mean value of 3 K, this corresponds to

Corresponding author address: Dr. Brian J. Soden, Rosenstiel School for Marine and Atmospheric Science, University of Miami, 4600 Rickenbacker Causeway, Miami, FL 33149.
E-mail: b.soden@miami.edu

Global Temperature Anomaly 1850-2016 © MET Office



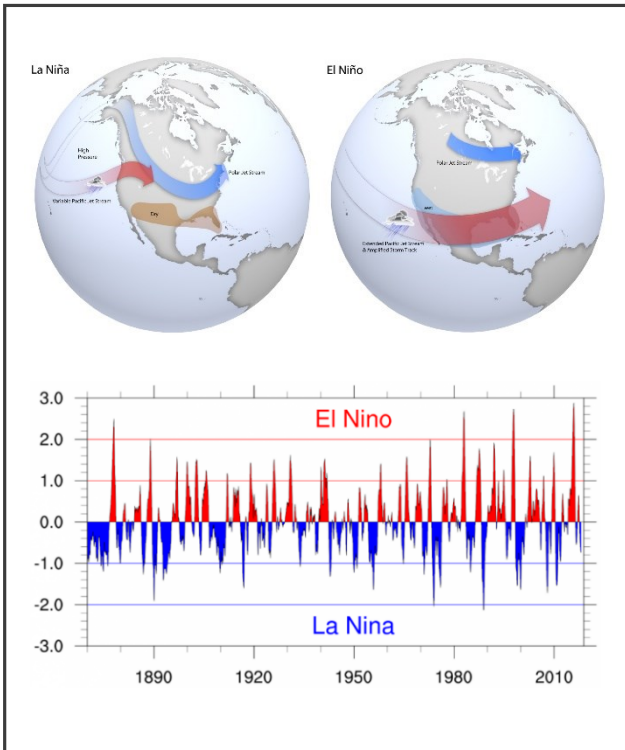
Secular Trend or Cyclical Variability



Held and Soden (2006)

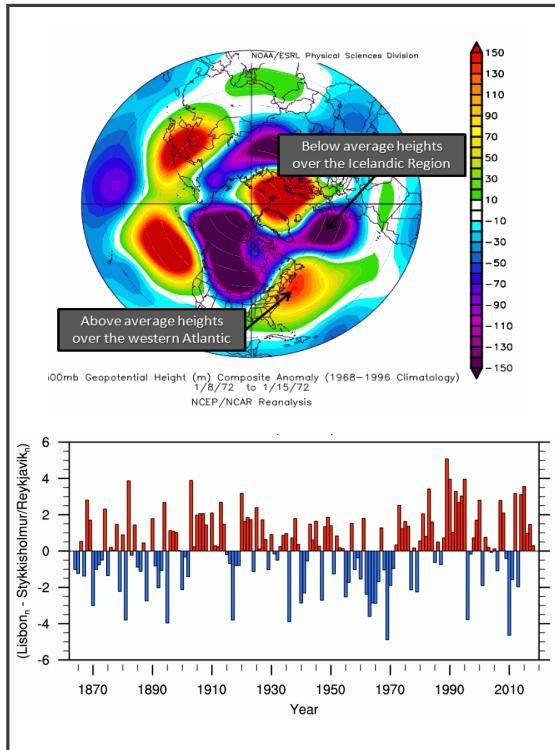
The Manifestation of Natural Climate Cyclicity

Data and Visualization © NOAA – National Weather Service



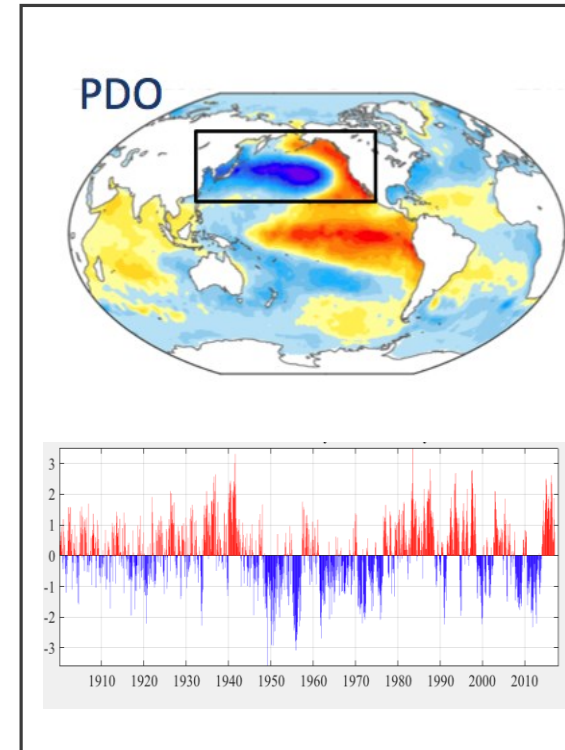
ENSO

a periodic fluctuation in sea surface temperature (Pacific Ocean)



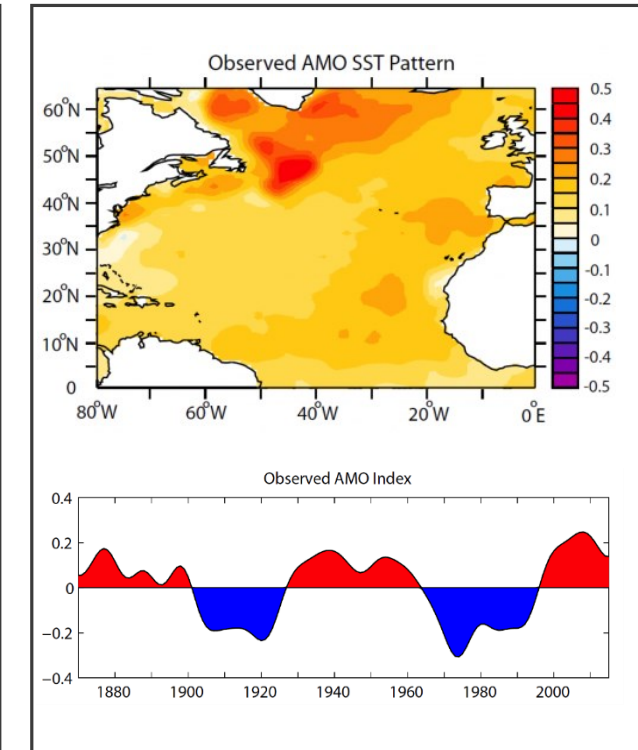
NAO

a periodic fluctuation in sea surface pressure (Atlantic Ocean)



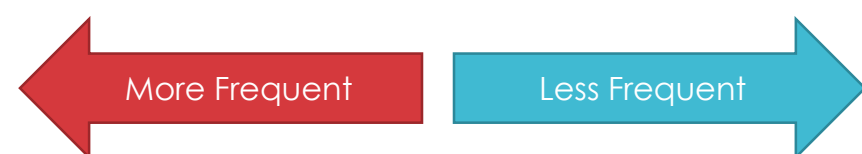
PDO

A long periodic fluctuation in sea surface temperature (Pacific Ocean)

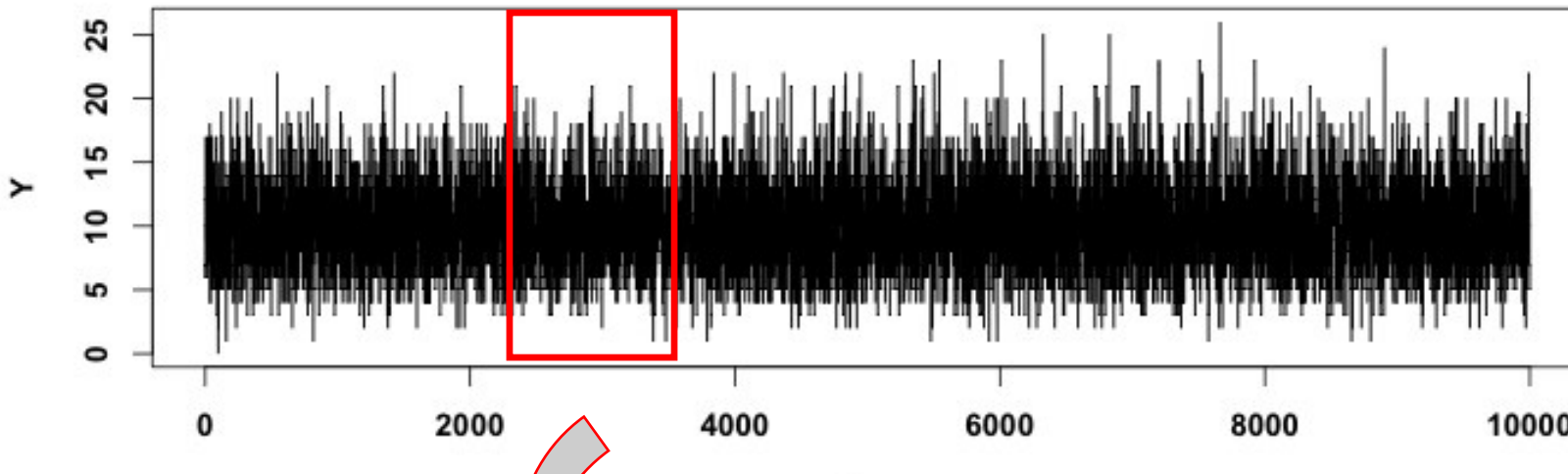


AMO

A long periodic fluctuation in sea surface temperature (Atlantic Ocean)



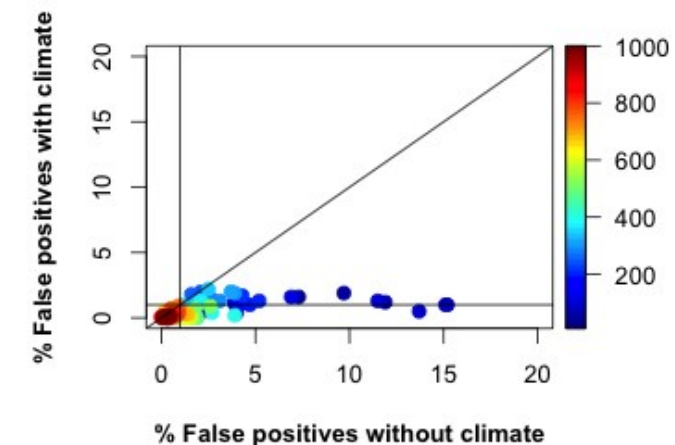
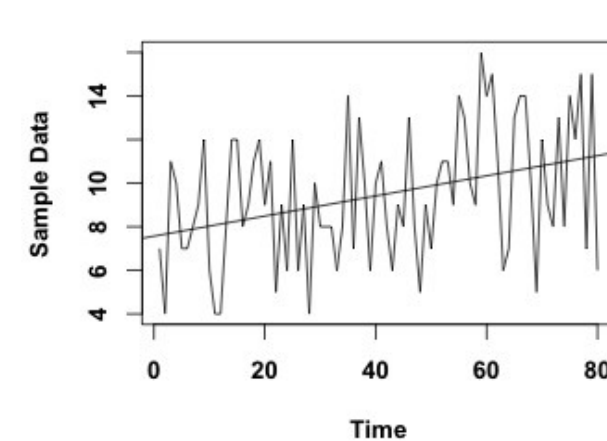
Learning from the Data and Attribution to Climate Modes



$$Y_i \sim \text{Poisson}(\lambda)$$

$$M_1: \lambda = \alpha + \beta_1 \cdot T + \text{error}$$

$$M_2: \lambda = \alpha + \beta_1 \cdot T + \beta_2 \cdot \text{Sin}(w_{T=5}) + \beta_3 \cdot \text{Sin}(w_{T=10}) + \beta_4 \cdot \text{Sin}(w_{T=20}) + \beta_5 \cdot \text{Sin}(w_{T=100}) + \text{error}$$



Synthetic data: Poisson process

Block of (10~1000) years

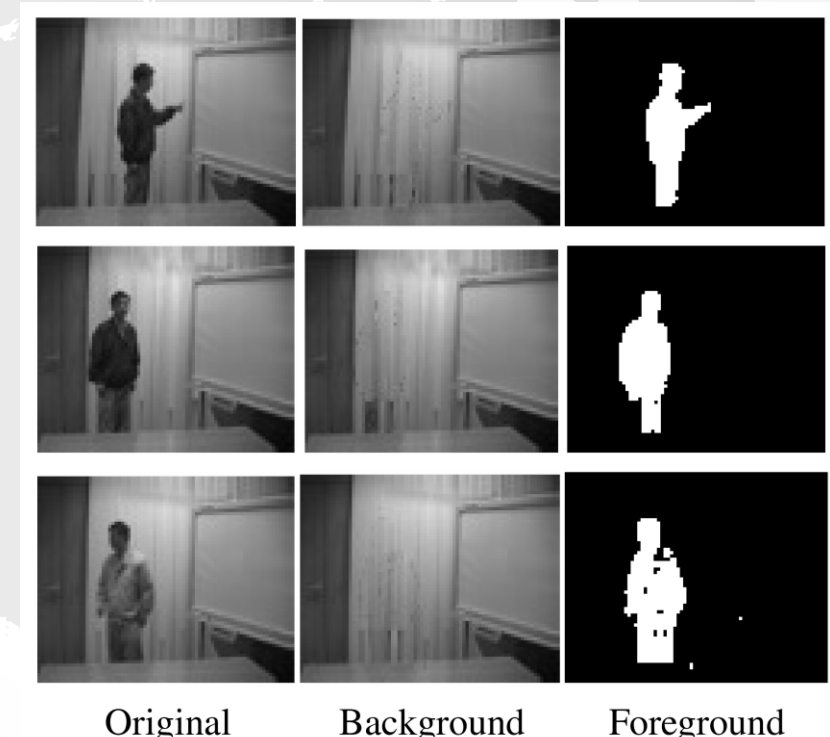
M1,M2 | 1% confidence level

Robust Component Analysis (RPCA) : Curse of Dimensionality and Outliers!

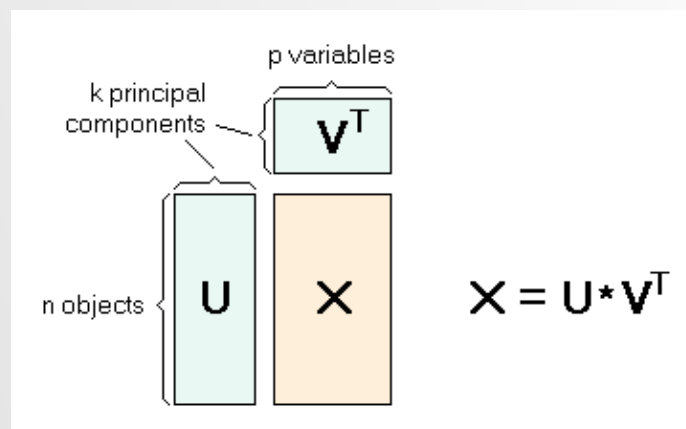
The algorithm split matrix to $M = L_0 + S_0$ where L_0 is low rank and S_0 is sparse

The algorithm Minimizes $\|L\|_* + \lambda \|S\|_1$ subject to $L + S = M$

The algorithm seeks the best rank-k estimate of L_0

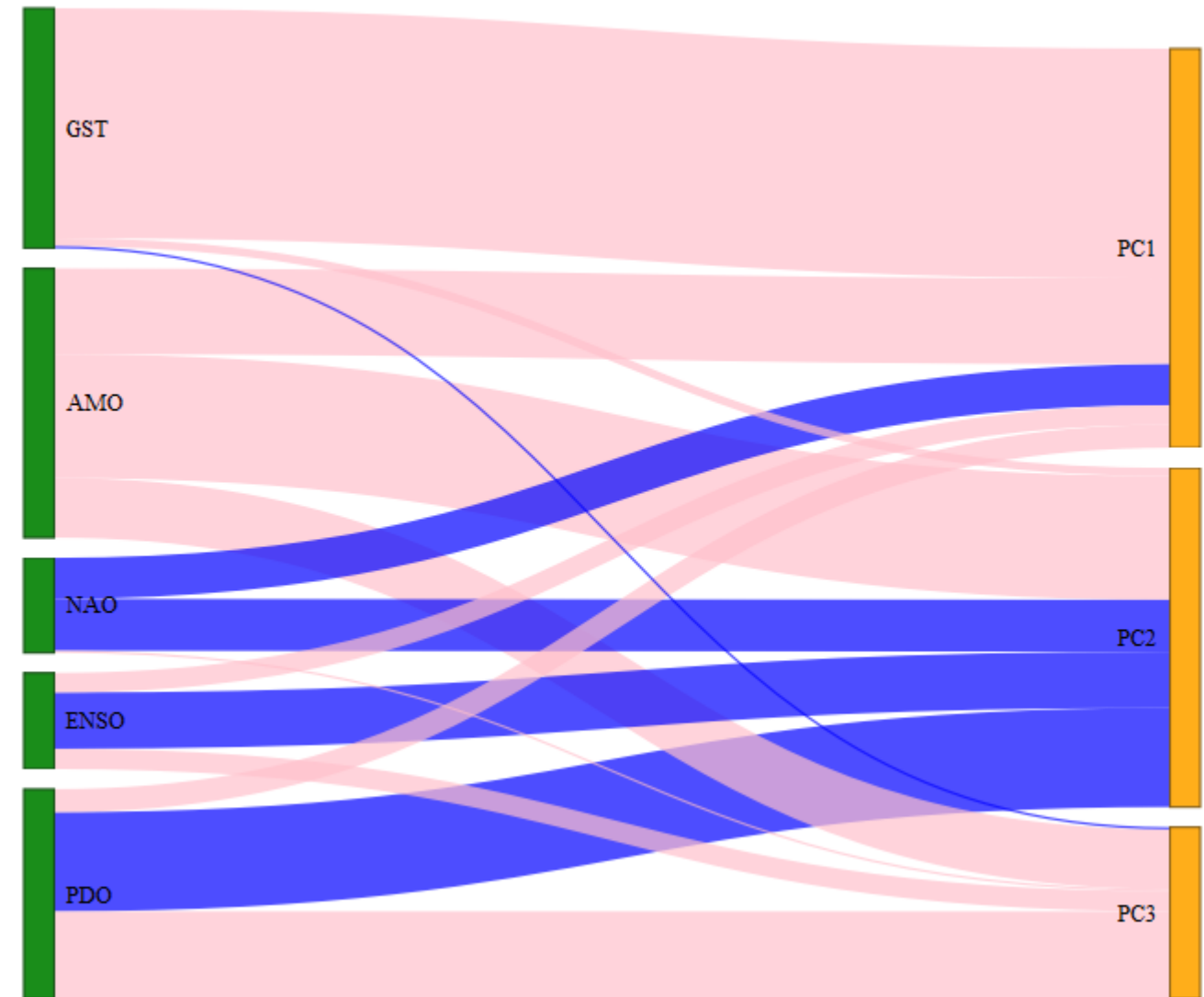
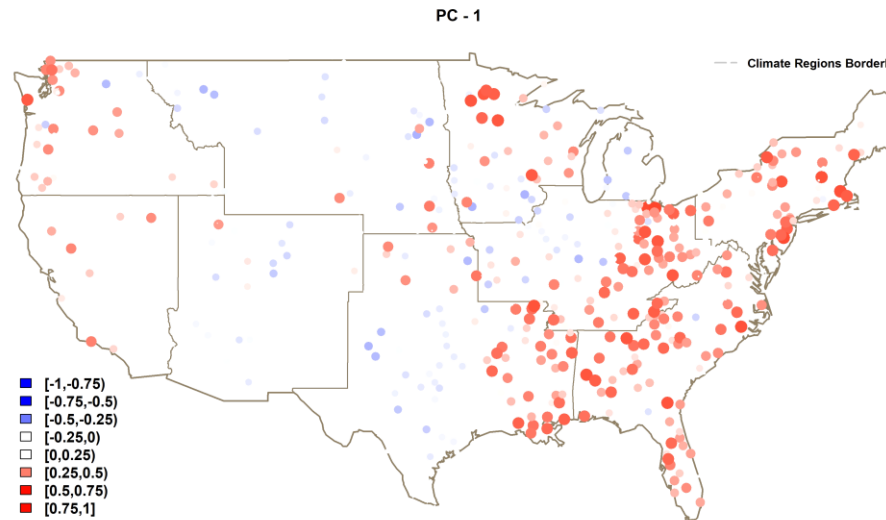
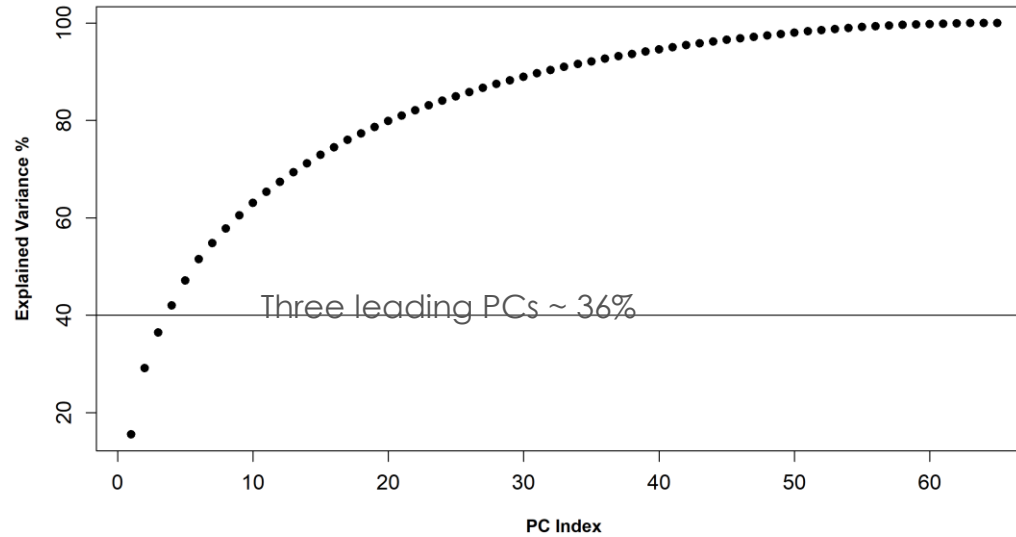


Dimension Reduction



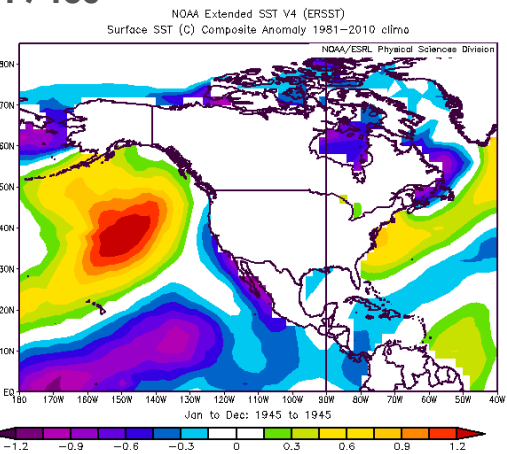
The V-Matrix is usually called the loadings matrix, and the U-Matrix is called the scores matrix

Robust Component Analysis (RPCA) on Annual Maximum Dry Periods

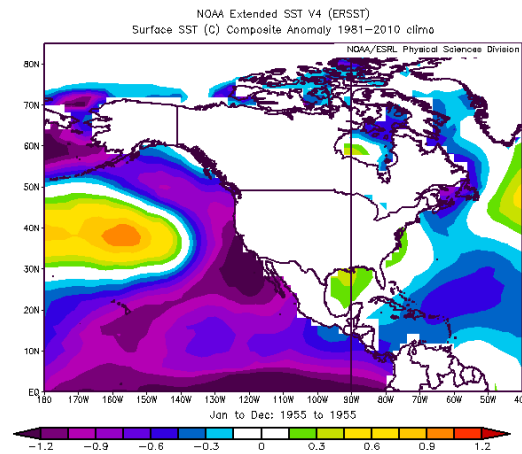


Correlation between Climate Indices and PCs

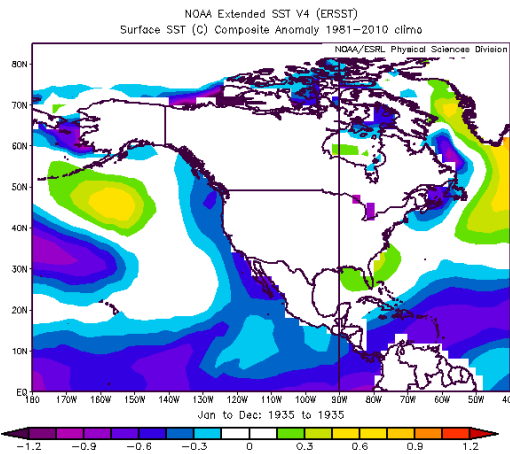
1940s



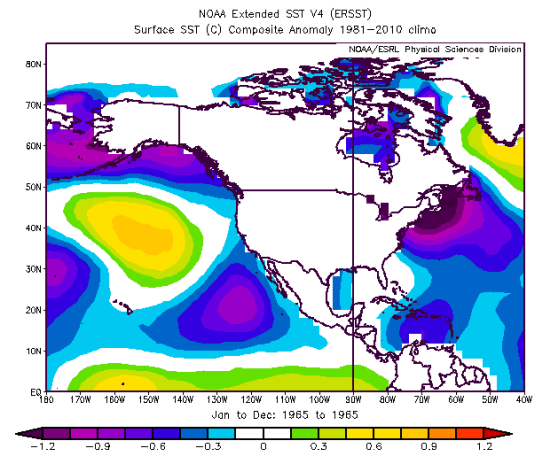
1950s



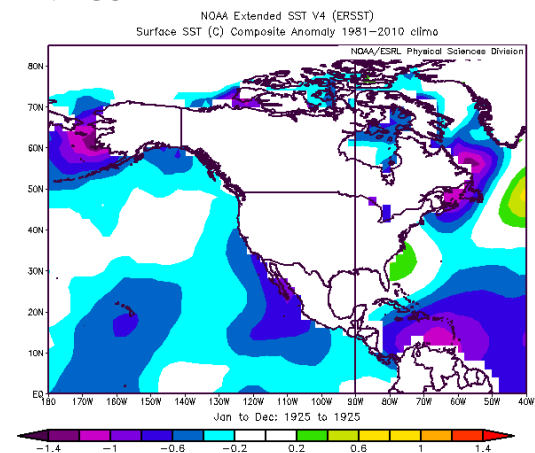
1930s



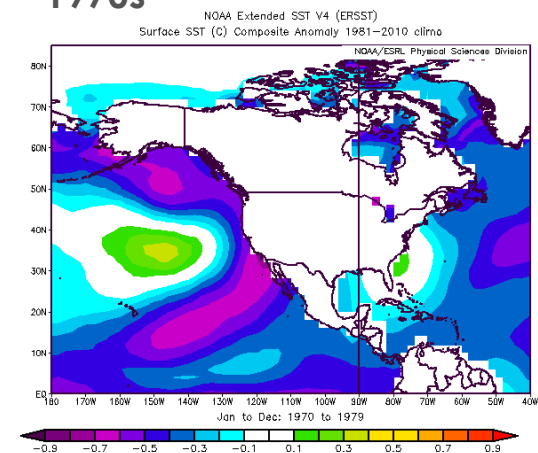
1960s



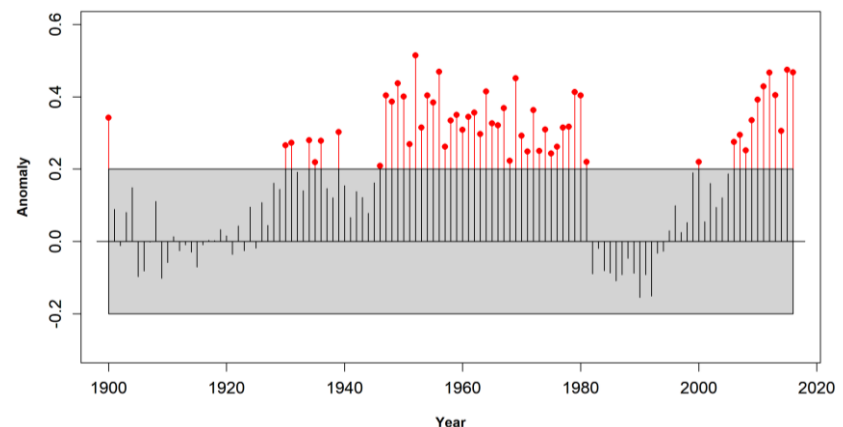
1920s



1970s



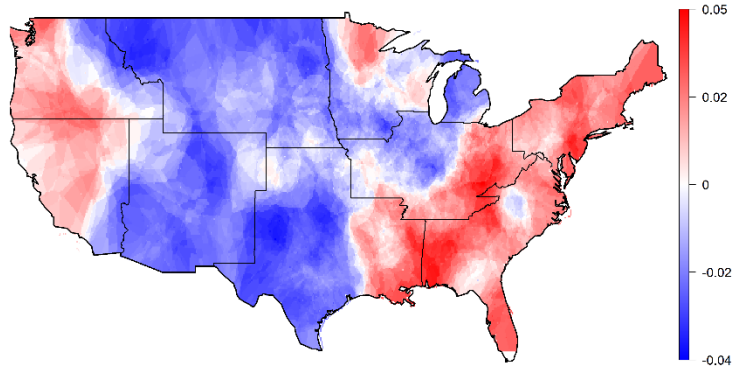
Anomaly of Sea Surface Temperature



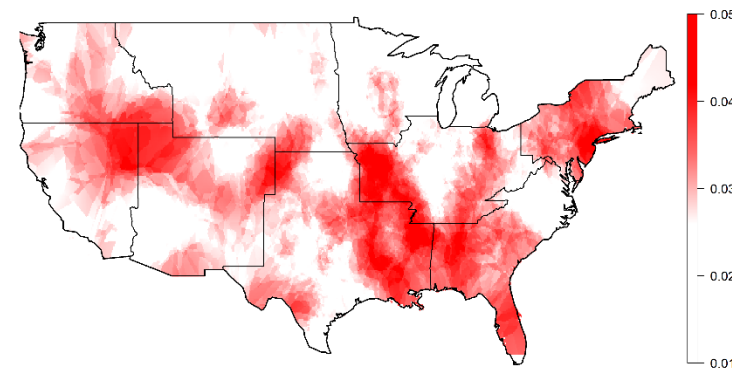
$$\text{Anomaly} = \text{Std.}(S) - \text{Std.}(L) / \text{Std.}(L)$$

Robust Component Analysis (RPCA) on Annual Maximum Dry Periods

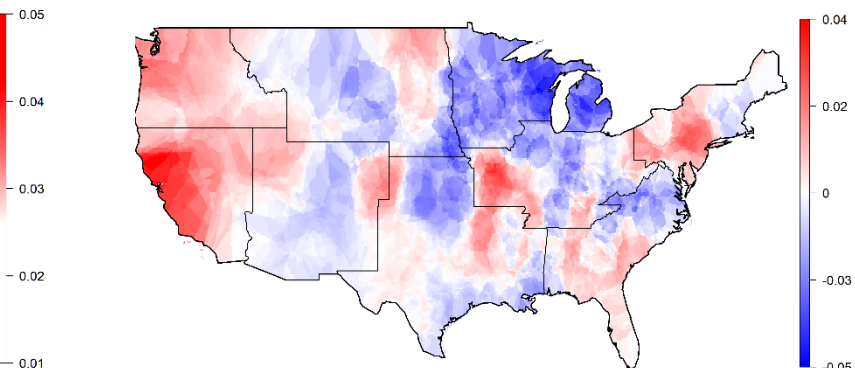
Loadings



PC1 – 15%

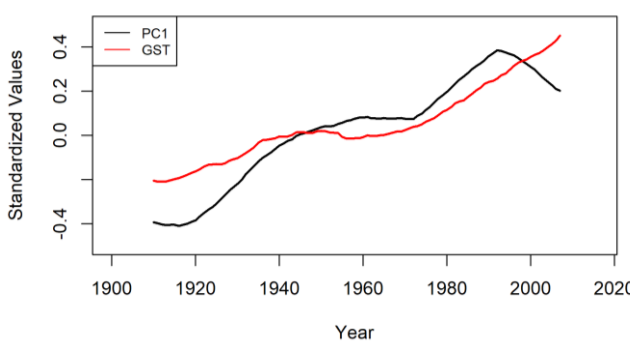


PC2 – 13.5%

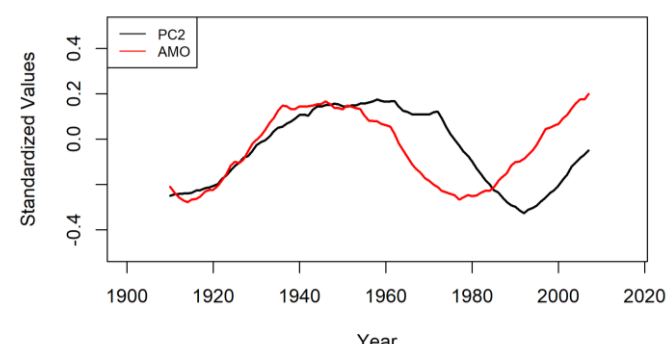


PC3 – 7%

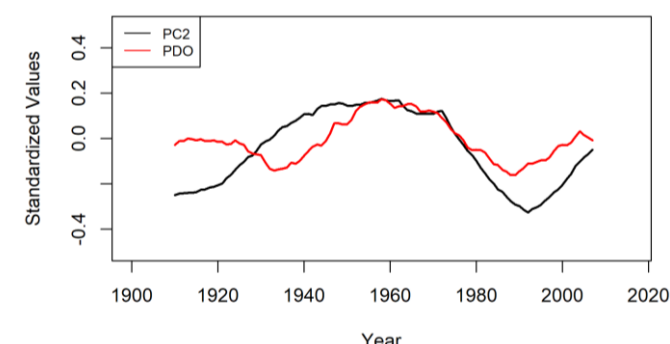
Scores



PC1 and GST



PC2 and AMO

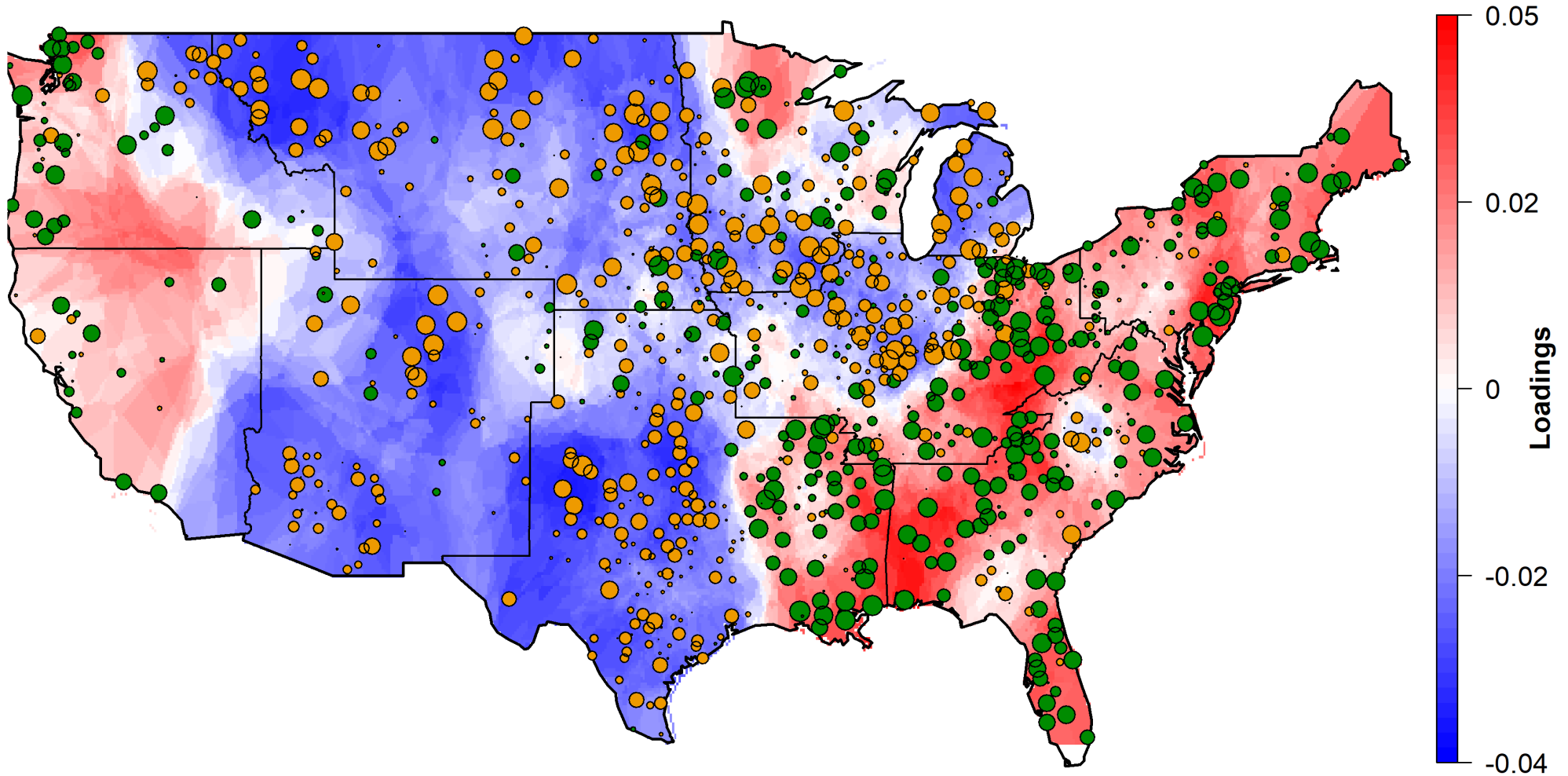


PC2 and -PDO

— Negative Trend
— Positive Trend

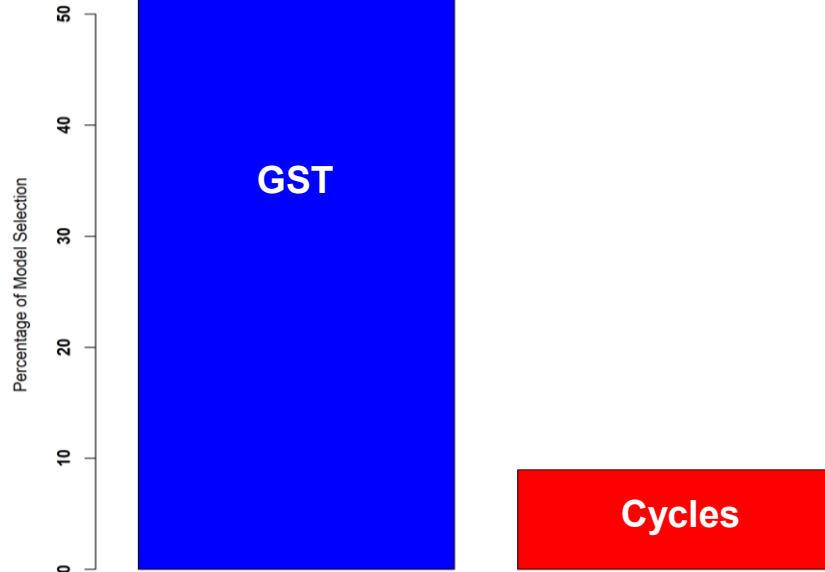
PC 1 Loadings

— Climate Regions Borderline



The loading map shows three main cluster across U.S.

The Points present the Kendall's tau coefficient at 0.05 Significance



$M_1 \sim GST$

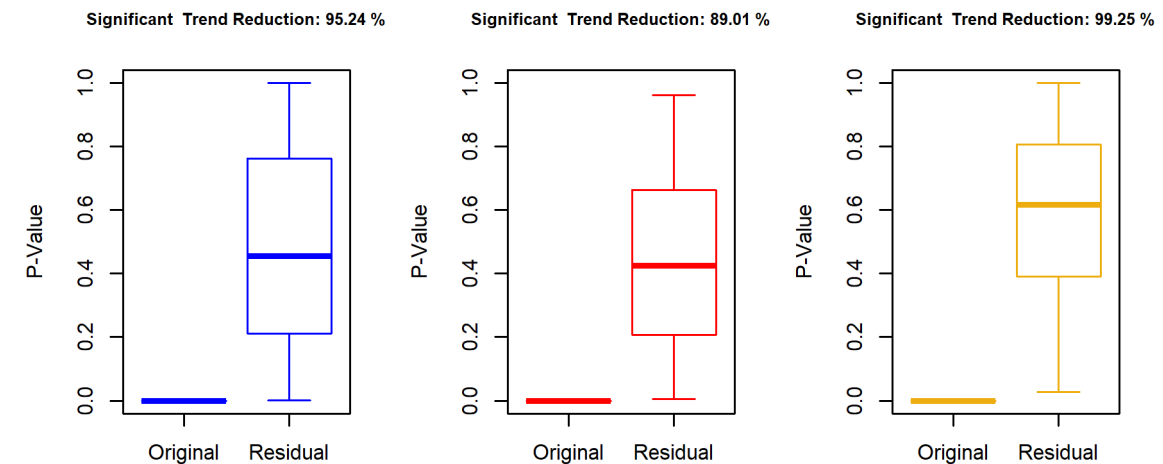
$M_2 \sim ENSO + NAO + PDO + AMO$

$M_3 \sim GST + ENSO + NAO + PDO + AMO$

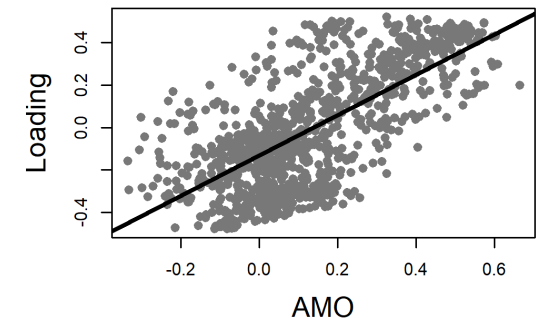
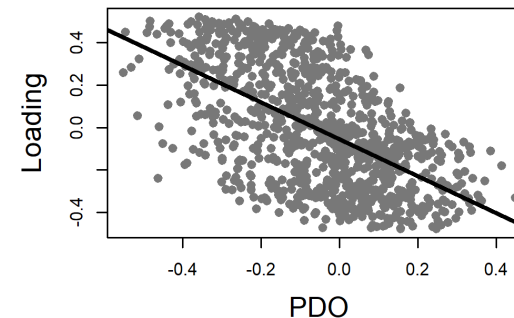
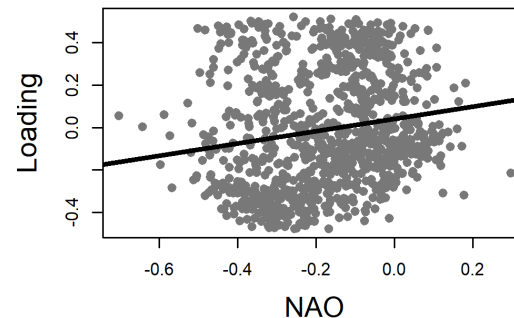
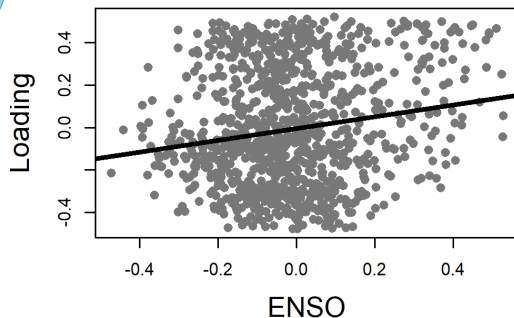
Check the model performance based on $AIC = 2k - 2 \ln (L)$

Considering the null hypothesis of no trend in residual of the model

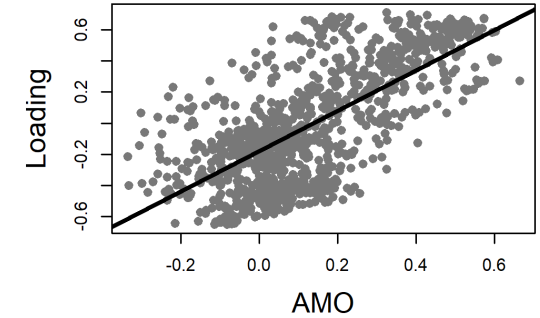
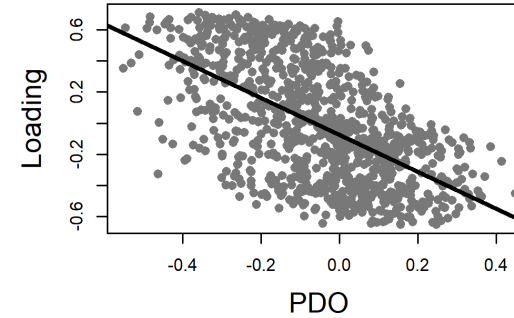
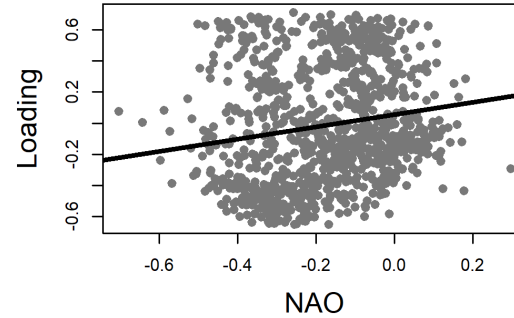
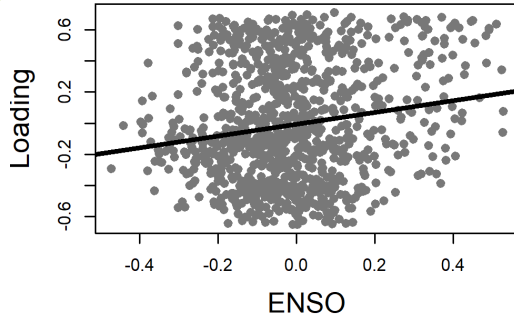
The Role of Different Climate Indices on Informing the Trends



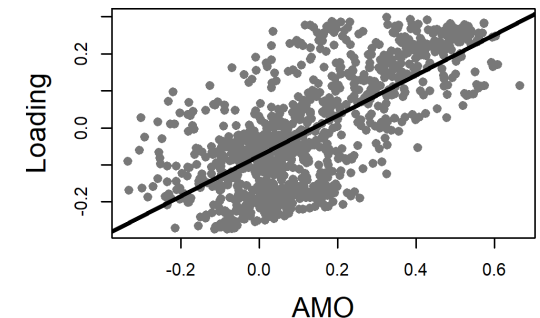
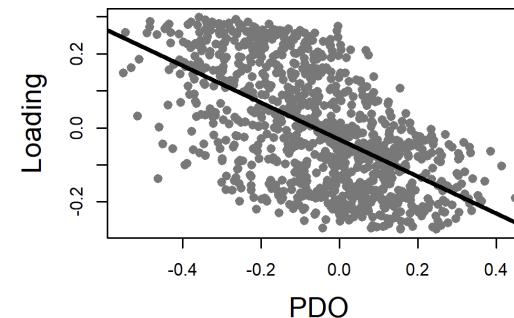
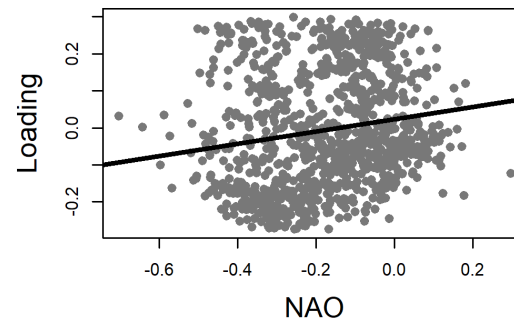
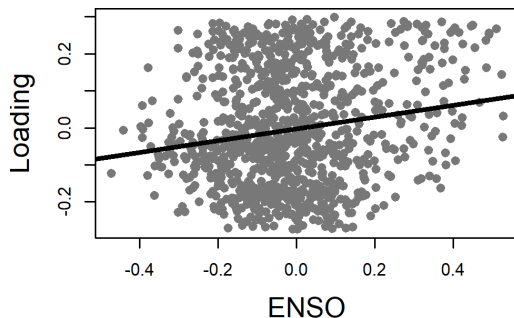
PC1



PC2

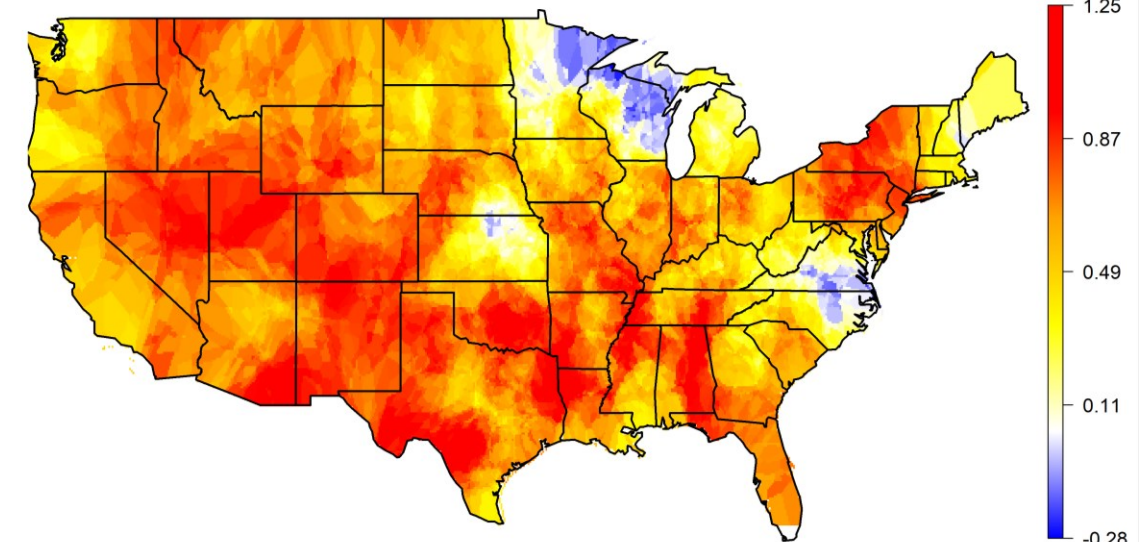


PC3



The association of Loading values from (standardized!) leading PCs with Climate Cycle Indices

Enhanced Dry Risk During Positive Phase AMO



State	AMO	PDO	Rank in US Agriculture
Texas	○	○	4
Kansas		○	7
Indiana		○	9
Ohio		○	11
Missouri	○		13
Arkansas	○		15
Florida		○	19
Colorado	○	○	20
Oklahoma	○	○	22
Mississippi	○	○	24
Alabama	○		25
Kentucky		○	27
Louisiana		○	29
New Mexico	○	○	30
Arizona	○		31
Utah	○		37
Nevada	○		42

Enhanced Dry Risk During Negative Phase PDO

